# Biomolecular mimicry in the actin cytoskeleton: Mechanisms underlying the cytotoxicity of kabiramide C and related macrolides

**Junichi Tanaka*†, Yuling Yan‡, Jeongeun Choi*, Jihong Bai*, Vadim A. Klenchin§, Ivan Rayment§, and Gerard Marriott*¶**

*Department of Physiology, University of Wisconsin, 1300 University Avenue, Madison, WI 53706; †Department of Chemistry, Biology, and Marine Science, University of the Ryukyus, Nishihara, Okinawa 903-0213, Japan; ‡Department of Mechanical Engineering, University of Hawaii at Manoa, Honolulu, HI 96822; and §Department of Biochemistry, University of Wisconsin, Madison, WI 53706

Edited by James A. Spudich, Stanford University School of Medicine, Stanford, CA, and approved August 13, 2003 (received for review June 4, 2003)

**This study characterizes the interactions between kabiramide C (KabC) and related macrolides and actin and establishes the mechanisms that underlie their inhibition of actin filament dynamics and cytotoxicity. The G-actin–KabC complex is formed through a two-step binding reaction and is extremely stable and long-lived. Competition-binding studies show that KabC binds to the same site on G-actin as Gelsolin domain 1 and CapG. KabC also binds to protomers within F-actin and results in the severing and capping of the (+) end; these studies suggest that free KabC and related macrolides act as biomimetics of Gelsolin. The G-actin–KabC complex binds to the (+) end of a growing filament, where it functions as a novel, unregulated, (+)-end capper and is largely responsible for the inhibition of motility and cytokinesis in ≈10–100 nM KabC-treated cells. KabC and related macrolides are useful probes to study the regulation of the actin filament (+) end and may lead to new therapies to treat diseases of the actin cytoskeleton.**

Motility is essential for cell survival and underlies the wound healing response, the neutralization of bacteria by neutrophils and tumor metastasis (1, 2). Some of the most dramatic events in cell protrusion occur in the lamellipodium, an ≈200- to 500-nm sheet of cytoplasm that extends and retracts in response to external cues that activate signaling pathways. Lamellipodial protrusion is linked to the rapid polymerization of a population of actin filaments from their (+) ends (3, 4). In resting cells, the (+) end of the actin filament is prevented from elongating through a specific interaction with one of three capping proteins, Gelsolin, CapG, and capping protein (reviewed in ref. 5). A transient increase in phosphatidylinositol 4,5-bisphosphate during cell signaling dissociates these capping proteins and exposes free (+) ends, which undergo rapid Arp2/3-mediated dendritic growth (6). The essential role of (+)-end-capping proteins is highlighted by Witke *et al.* (7), who showed that macrophage cells derived from CapG/Gelsolin double-null mice exhibit diminished membrane ruffling and cell protrusion.

The molecular regulation of cell protrusion is a complex process involving as many as 100 different proteins and signaling molecules. To understand how the activities of these biomolecules are temporally and spatially regulated within the lamellipodium, we need to develop new molecular tools and techniques to specifically perturb and monitor molecular interactions of G-actin and actin filaments (8–10).

In this report we establish the actin-binding modes and inhibitory mechanisms for a family of cytotoxic marine natural product macrolides. These drugs can be classified as (*i*) macrolides that usually contain a trisoxazole group and are typified by kabiramide C (KabC) (refs. 11 and 12 and Fig. 1) and Ulapualide A (UlaA; Fig. 1 and ref. 13) or (*ii*) dimeric macrolides such as Swinholide A (SwiA) (14, 15). Previous studies suggest that certain macrolides inhibit actin polymerization by sequestering actin monomers and sever actin filaments (12, 15), whereas SwiA is thought to sequester actin dimers during the nucleation phase of filament growth (14), and misakinolide A (MisA) (16) is purported to bind to the actin dimer at the (+) end of the filament. However, evidence presented in this article suggests that the inhibitory and cytotoxic effects of KabC and related macrolides are mediated through a unique actin-binding modes and novel mechanisms. The findings of this study are supported, in part, by a recent investigation defining the structural basis for the interaction of macrolides with G-actin (17). These structural studies show that the complex is formed through hydrophobic interactions between the macrolide ring of KabC with

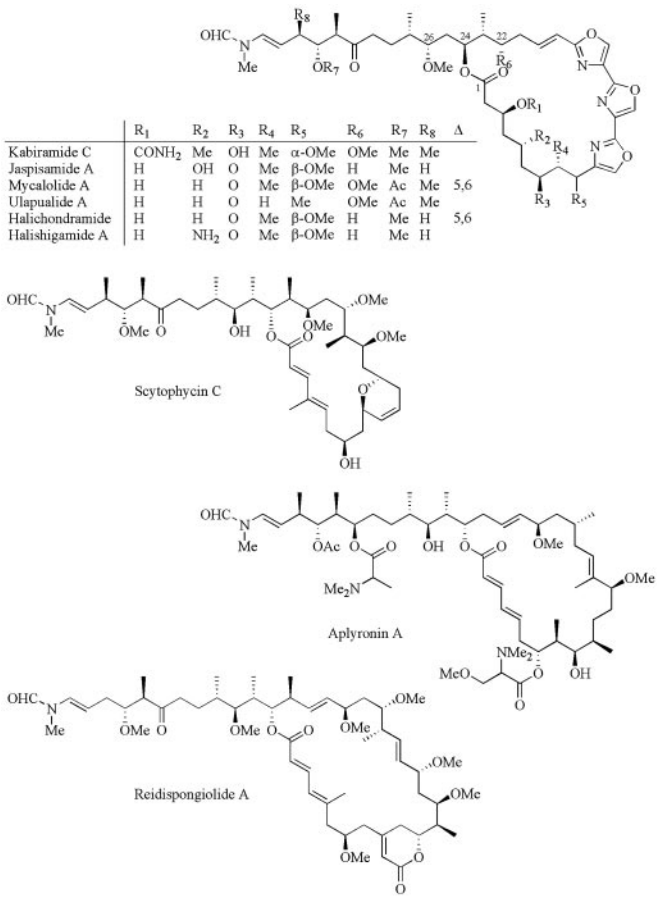


**Fig. 1.** Molecular structure of kabiramide and related trisoxazole macrolides studied in this work as well as structures of related macrolides.

BIOCHEMISTRY

This paper was submitted directly (Track II) to the PNAS office.

Abbreviations: KabC, kabiramide C; UlaA, Ulapualide A; MisA, misakinolide A; GS1, Gelsolin domain 1.

¶To whom correspondence should be addressed. E-mail: gm@physiology.wisc.edu.

a surface patch close to subdomains 1 and 3 of actin and the KabC tail within the deep cleft that forms at the interface of these two subdomains. In this study we present a detailed analysis of the different binding modes of KabC to G-actin and show how these interactions are responsible for KabC-mediated inhibition of actin filament dynamics and cytotoxicity. The functional studies reported in this article and in the study by Klenchin *et al.* (17) suggest that free KabC acts as a novel biomimetic of Gelsolin, whereas the stable G-actin–KabC complex acts as a novel, unregulated (+)-end-capping protein complex.

## Materials and Methods

**Cell Culture.** Rat bladder NBT-II cells and mouse NIH 3T3 cells are used as described by Choidas *et al.* (18).

**Fluorescence Spectroscopy.** A customized SLM-Aminco AB2 fluorometer is used to record fluorescence emission and excitation spectra. Emission spectra are corrected for the instrument response as described by Marriott *et al.* (19).

**Live Cell Microscopy.** A microscope workstation is used to image phase contrast and fluorescence images of living cells as described by Choidas *et al.* (18).

**Isolation and Purification of Macrolide Drugs.** KabC is purified from the black sponge *Ircinia* sp. collected off Sichang Island in the Gulf of Thailand and identified on the basis of $^{1}H$ and $^{13}C$ NMR spectra. Halichondramide is purified from an unidentified black sponge collected off Iriomote Island in Okinawa. LatA, MisA, and SwiA are isolated from marine sponges as described by Jefford *et al.* (20), Kobayashi *et al.* (21), and Tanaka *et al.* (22). P. J. Scheuer (deceased) from the University of Hawaii provided the sample of purified UlaA.

**Cloning and Gene Expression.** Mouse Gelsolin and CapG genes are amplified by PCR using a mouse brain cDNA library (Invitrogen) as a template and gene specific primers and cloned in the *Hin*dIII, *Bam*HI site of the pQE30 vector that has an N-terminal His-tag. DNA sequencing confirmed the sequence of genes. The M15 bacterial strain is used to express the genes.

**Protein Purification.** A 1.6-liter culture of bacteria expressing genes for CapG, Gelsolin, or Gelsolin domain 1 (GS1) is induced with 1 mM isopropyl β-D-thiogalactoside at 30°C or 37°C for 5–6 h (Fig. 2*A*), then harvested and lysed by using a combination of lysozyme and sonification on ice. All of the expressed proteins are soluble, and the purification is carried out by using nickel-nitrilotriacetic acid (Qiagen). About 50 mg of pure CapG is purified from a 600-ml culture.

**F-Actin.** F-actin is purified from rabbit skeletal muscle by using a standard protocol developed in the Marriott laboratory (19). The purity and activity of actin is analyzed by using SDS/PAGE, polymerization assays, and a motility assay (23).

**Prodan-Actin.** Actin is labeled with the thiol probe, Acrylodan (Molecular Probes) by using a standard protocol described by Marriott *et al.* (19). Prodan-actin behaves as unlabeled actin in all functional assays tested (9, 19, 24).

**Determination of the Binding Stoichiometry and Dissociation Constants for G-Actin Complexes with Actin-Binding Proteins and Macrolide Drugs.** The stoichiometry of the CapG–G-actin and macrolide–G-actin complex is determined by titrating Prodan-G-actin at 1 μM with increasing amounts of CapG or the macrolide from 0.1 to 10 μM. The equilibrium binding constant is determined by titrating a constant amount of Prodan labeled G-actin at ≈0.05–0.1 μM in G or F buffer (19) with incrementally increasing amounts of the macrolide or CapG over a range of 10 nM to 10 μM. Control experiments show that the addition of up to 2% methanol to Prodan-G-actin has no effect on the emission spectrum or polymerization kinetics. The thermodynamic parameters for the equilibrium are determined from an analysis of these binding data by using a standard binding algorithm (25).

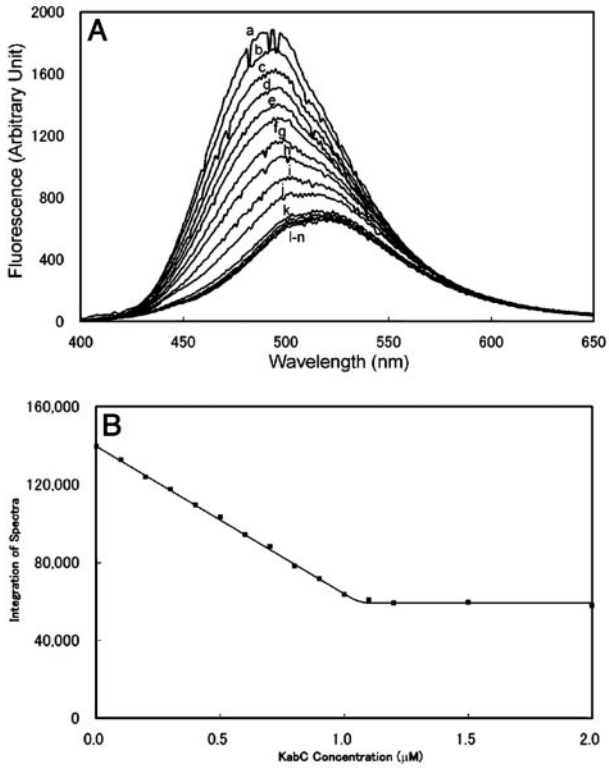


**Fig. 2.** (*A*) Stoichiometric binding of Prodan-labeled G-actin (1 μM) in G buffer with KabC at final concentrations of (in μM) 0.0 (trace a); 0.1 (trace b); 0.2 (trace c); 0.3 (trace d); 0.4 (trace e); 0.5 (trace f); 0.6 (trace g); 0.7 (trace h); 0.8 (trace i); 0.9 (trace j); 1.0 (trace k); 1.1 (trace l); 1.2 (trace m); and 1.5 (trace n). (*B*) Plot of the integrated intensity in *A* against [KabC] yields a binding stoichiometry of 1:1.

**Kinetic Analysis of Binding Reactions.** The kinetics of the KabC interaction with Prodan-actin is determined, by using an Applied Photophysics SX.18MV stopped-flow spectrometer, by following the decrease in the emission intensity of Prodan-actin at 25°C. Prodan is excited at 385 nm, and emission is collected with a 470 nm (±5 nm) band-pass filter. In all cases, the decrease in emission intensity is best fit with a single exponential function, which is then used to determine the observed rate, $k_{obs}$. Kinetic constants of on rate ($k_{on}$) and off rate ($k_{off}$) are calculated according to the following equation: $k_{obs} = k_{on}[\text{KabC}] + k_{off}$. The kinetics of the slower binding step observed in the interaction of KabC with Prodan-G-actin interaction is determined by measuring the ratio of fluorescence signals at 465 and 530 nm. The decay of this ratio is fit by using a single exponential rate.

**Prodan-Actin Polymerization Assay.** Polymerization of a 5 μM solution of Prodan-labeled G-actin is initiated by adding KCl and $MgCl_2$ to 100 and 2 mM, respectively, and the time course of the reaction is monitored by recording the emission intensity at 465 nm. In other experiments, the progress of actin polymerization is determined by recording the Prodan-actin emission spectrum at defined times during the reaction.

**Characterization of Actin-Binding Proteins.** The actin-binding properties of the actin-binding proteins used in this study are

evaluated from changes in the fluorescence emission spectrum of Prodan-actin and actin polymerization assays as described by Marriott *et al.* (19).

## Results and Discussion

**High-Resolution Structures of G-Actin Bound to KabC and Jaspisamide A (JspA).** In a recent article (17), we described high-resolution structures of G-actin complexes with KabC and JspA (this is unrelated to the F-actin-binding drug, jasplakinolide) at a resolution of 1.45 and 1.6 Å, respectively. In summary, these structural studies show that KabC and JspA mediate their interactions with actin through hydrophobic contacts involving two distinct structural moieties in the KabC molecule. (*i*) The macrolide ring, which exhibits a considerable variation in ring size and side groups, is firmly attached to surface of actin at the interface of subdomains 1 and 3 through hydrophobic contacts with Ile-341, Ile-345, Ser-348, and Leu-349. Most of the polar side groups in the macrolide ring are directed toward the solvent while hydrophobic groups engage in specific apolar interactions with hydrophobic residues in actin. (*ii*) A long hydrophobic tail, which is conserved in length and the stereochemistry of its side groups, that binds deeply within the cleft between subdomains 1 and 3. The contacts made between the KabC tail and the actin cleft are primarily hydrophobic with major contributions from actin at residues Tyr-143, Gly-146, Thr-148, Gly-168, Tyr-169, Ile-345, Leu-346, Thr-351, Met-355, and Phe-375. The cleft region is also critical for the interaction of G-actin with GS1 (26) and the axial actin protomer in the filament (17).

**Prodan-Actin: An Environmentally Sensitive Actin Conjugate.** Amino acid residues close to Cys-374 in actin are known to engage in specific interactions with structural elements of the (+)-end-capping proteins, CapG, capping protein, and GS1 (27). Fluorescence measurements of optical probes attached to Cys-374 of actin can provide key information on molecular complexes of actin with actin-binding proteins or drugs: Pyrene-actin (28, 29) and Prodan-actin (19) are the best-characterized conjugates. The fluorescence emission of Prodan-actin is sensitive to subtle changes in its molecular environment that results from actin-binding protein and/or drug binding (19, 24). For example, the average emission energy of Prodan in G-actin shifts from 496 nm (on a wavelength scale) for G-actin to 465 nm in F-actin. On the other hand, the binding of KabC to Prodan-G-actin decreases the quantum yield of the probe nearly 3-fold and shifts the emission to 520 nm (Fig. 2*A*). Similar spectral shifts are seen with other macrolides including swinholide and misakinolide (data not shown). The sensitivity of the Prodan in actin to KabC binding reflects its close proximity to the macrolide ring-binding site (17). On the basis of earlier spectroscopic studies (19, 30, 31), we suggest that this sensitivity arises from a KabC-induced change in a specific dipolar interaction between the Keto-oxygen or the substituted amine on the probe and a peptide dipole within the actin matrix, and/or, from a general solvent effect associated with an increased exposure of the probe to the solvent.

The macrolide-mediated red-shift in the emission of Prodan-G-actin is used to determine key thermodynamic and kinetic parameters for this interaction. For example, KabC, UlaA, and Hal all bind to G-actin with a stoichiometry of 1:1 and exhibit a dissociation constant of 100 nM or less (Fig. 2). A determination of a true dissociation constant is difficult because KabC binds to G-actin in a complex two-step reaction as described below.

**KabC and Other Trisoxazole Macrolides Bind to Prodan-G-Actin in a Two-Step Reaction.** The kinetic parameters describing the interaction of Prodan-G-actin with KabC are determined by analyzing the decrease in fluorescence intensity at 480 nm. The initial interaction, which accounts for most of the quenching and red-shift in Prodan-actin fluorescence, occurs at a rate of 30 $sec^{-1}$ (Fig. 3 *A* and *B*).

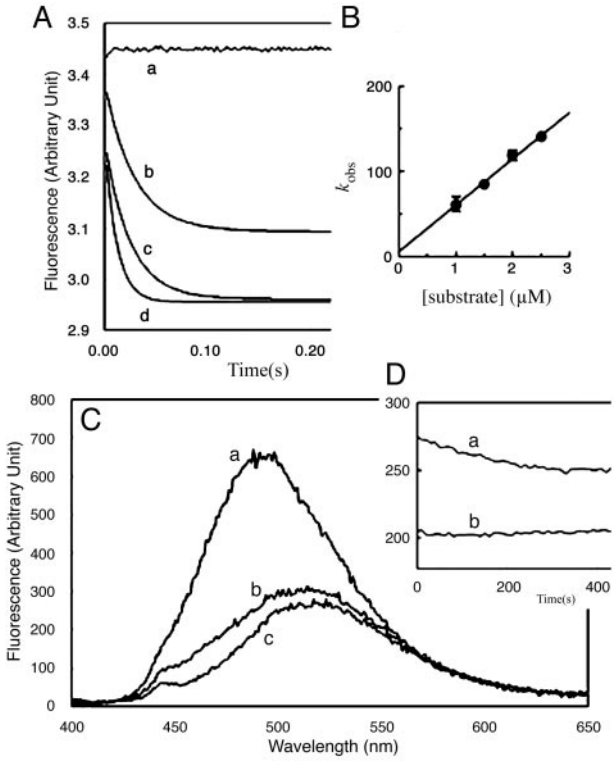


**Fig. 3.** Kinetic analyses of KabC binding of Prodan-labeled G-actin. (*A* and *B*) Stopped-flow data recorded in the lab of E. R. Chapman. Prodan-actin (0.1 $\mu$M) and KabC, loaded into separated syringes, were rapidly mixed within ≈1 msec of dead time. The concentrations of KabC were 0.0 $\mu$M (trace a), 1.0 $\mu$M (trace b), 1.5 $\mu$M (trace c), 2.0 $\mu$M (trace d), and 2.5 $\mu$M (data not shown). The observed rates are plotted as a function of the [KabC] in *B*. The *y*-intercept and the slope yield $k_{off}$ (5.6 ± 5.9 $sec^{-1}$) and $k_{on}$ (54.5 ± 3.2 × $10^6$ $M^{-1}$·$sec^{-1}$), respectively. These kinetic constants give rise to a ''dissociation constant'' of ≈0.1 $\mu$M. (*C*) The emission spectrum of 0.1 $\mu$M Prodan-G-actin (trace a); soon after adding KabC (trace b); and after a further 5 min (trace c). (*D*) Kinetics of the slower binding step monitored through the decrease at 465 nm (trace a) with respect to 550 nm (trace b).

Interestingly, the emission of the Prodan-actin–KabC complex shows a second, slower decrease in quantum yield and red-shift that evolve at a rate close to 0.008 $sec^{-1}$ (Fig. 3*D*). Related studies using Hal and UlaA suggest that the first and second binding steps are common to all trisoxazole macrolides (data not shown). Dilution and competition-binding studies show that the final G-actin–KabC complex is extremely stable and does not dissociate at a concentration below the dissociation constant of 100 nM, as might be expected for a simple binding reaction. This property can be rationalized if the second binding step serves to kinetically trap the macrolide within the actin matrix. Because we know that the initial binding event is rapid and accounts for most of the fluorescence quenching, it seems likely the second, slower binding step involves the interaction of the long KabC tail within the actin matrix. This assignment is consistent with an analysis of the KabC-actin structure, which shows the tail binds deeply within the cleft. Furthermore, a structural analysis of all of stabilizing bonds in the KabC-G-actin complex suggests that the tail contributes a significant amount to the total binding energy (17).

**Trisoxazole Macrolides Specifically Compete with GS1 for the (+)-End-Binding Site on Actin.** Gelsolin exerts two major effects once bound to an actin filament: (*i*) it severs the filament, and (*ii*) it remains tightly bound to the severed (+) end and serves to block, or cap, further growth (32). The complex between Gelsolin and the (+) end is very strong although it can be dissociated by

BIOCHEMISTRY

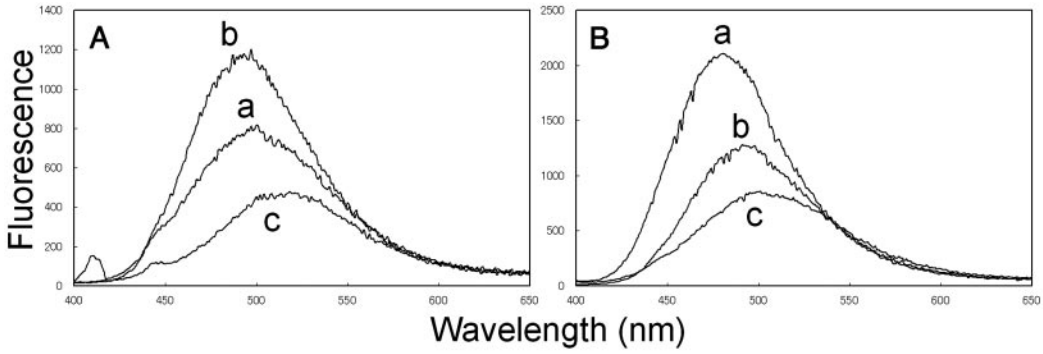


**Fig. 4.** (*A*) CapG: Prodan-G-actin (100 nM, trace a) and Prodan-G-actin-CapG (trace b); trace c is the same as trace b but in the presence of 0.2 $\mu$M KabC. (*B*) GS1: Prodan-G-actin (100 nM, trace a) and Prodan-G-actin-GS1 (trace b); trace c is the same as trace b but in the presence of 0.2 $\mu$M KabC.

phosphatidylinositol 4,5-bisphosphate (33, 34). Structural analyses of G-actin complexes with GS1 (26) and KabC reveal common contact sites that include a patch of hydrophobic residues on the surface between subdomains 1 and 3 and within the cleft between subdomains 1 and 3 (17, 26). GS1 shifts the average energy of Prodan-G-actin emission to the red and is accompanied by a decrease in the quantum yield (Fig. 4*A*), although not to the same extent as KabC–G-actin (Fig. 2). This difference is exploited in a competition-binding assay that shows KabC efficiently displaces GS1 from Prodan-G-actin in the presence of EGTA (Fig. 4*B*), but GS1 does not displace KabC from G-actin (data not shown), which is consistent with our finding that the KabC–G-actin complex is remarkably stable.

**Trisoxazole Macrolides Specifically Compete with CapG for the (+)-End Binding Site on Actin.** CapG, a $Ca^{2+}$-dependent, (+)-end-actin filament capping protein, is found at high levels in macrophage cells where it regulates membrane ruffling and cell protrusions (35). The $Ca^{2+}$-dependent binding of CapG to Prodan-G-actin is accompanied by a dramatic blue shift in the emission spectrum and an increase in quantum yield (Fig. 4*A*, trace b). The difference in fluorescence between free and CapG-bound Prodan-G-actin is used to show that the reversible complex has a stoichiometry of 1:1 and a dissociation constant of 100 nM (data not shown). Related competition-binding assays are used to show that, although KabC and related macrolides displace CapG from Prodan-G-actin in a $Ca^{2+}$-independent manner (Fig. 4*A*), CapG cannot displace KabC from G-actin and that GS1 displaces CapG from its complex with Prodan-G-actin. Together these data show that CapG, GS1, and KabC and related macrolides share a common binding site on G-actin. This conclusion is consistent with a comparison of the high-resolution structures of G-actin with GS1 and KabC (17) and our analysis of a preliminary 2.8-Å structure of a CapG mutant (PDB ID code 1JHW). Finally, this competition-binding assay is used to demonstrate that the dimeric macrolides, SwiA and MisA, also bind to the same site on G-actin as KabC, CapG, and GS1. However, the emission properties of the CapG–Prodan-G-actin complex are unaffected by the binding of LatA, DNase, and thymosin $\beta$4 (T$\beta$4) (data not shown), which is consistent with some structural data showing that these sequestering molecules bind to sites distant from subdomains 1 and 3 (36)

**The G-Actin–KabC Complex Inhibits Actin Polymerization by Capping the (+) End of the Filament.** Most actin monomer sequestering proteins and drugs, such as T$\beta$4 (9) and LatA (37) engage in short-lived interactions with G-actin. These complexes usually exhibit dissociation constants close to the critical concentration for actin polymerization (0.2 $\mu$M). On the other hand, the G-actin–KabC complex is extremely stable and has a very long lifetime. Here we show that the cytotoxicity of low concentrations of KabC (>10 nM) result from the stable G-actin–KabC complex. Specifically, we tested the hypothesis that KabC–G-actin acts as an unregulated, (+)-end-capping protein that prevents the incorporation of new actin monomers. We determined the rate of Prodan-G-actin polymerization in the presence of varying amounts of the preformed KabC–G-actin complex (from 1/5,000 to $\approx$1/20 of the total G-actin). The amount of G-actin sequestered by KabC in this mixture does not change the critical concentration for actin polymerization of 0.2 $\mu$M. Adding KCl and $MgCl_2$ to 100 mM and 2 mM polymerizes this G-actin mixture, and the reaction is monitored through the increase in fluorescence at 465 nm (Fig. 5 and ref. 19). These data show that trace levels of the G-actin–KabC complex reduce the rate and extent of actin polymerization (e.g., Fig. 5, trace e). We propose that the preformed G-actin–KabC mediates this effect by binding to actin dimers and trimers during the nucleation phase and/or by capping of the (+) end of filament during the elongation phase. On the basis of this study and in the study by Klenchin *et al*. (17), we propose that G-actin–KabC inhibits actin filament dynamics by acting as novel, unregulated, (+)-end-capping protein complex.

**KabC and Related Macrolides Bind to F-actin and Cause Filament Severing.** Previous fluorescence studies using Pyrene-labeled F-actin associate a macrolide-mediated decrease in pyrene fluorescence to actin filament severing (12, 14, 16). If true, then these macrolides must sever actin filaments in an extremely efficient manner. However, the assumption that the decrease in the pyrene

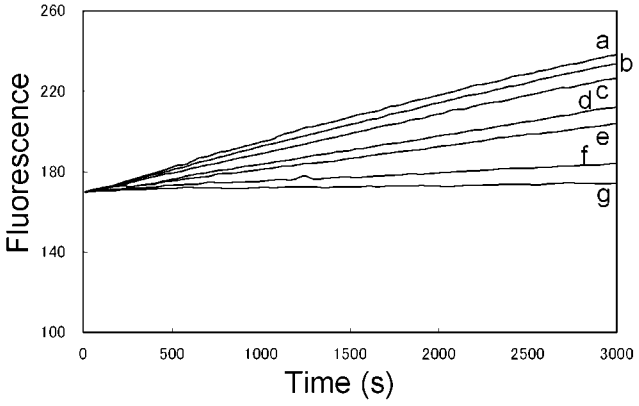


**Fig. 5.** Time course for G-actin polymerization. Prodan-labeled G-actin is mixed to a final concentration of 5 $\mu$M with preformed G-actin–KabC at 0 nM (trace a); 1 nM (trace b); 5 nM (trace c); 10 nM (trace d); 20 nM (trace e); 50 nM (trace f); or 250 nM (trace g), and the polymerization reaction was initiated by KCl and $MgCl_2$ to 0.1 M and 2 mM, respectively.

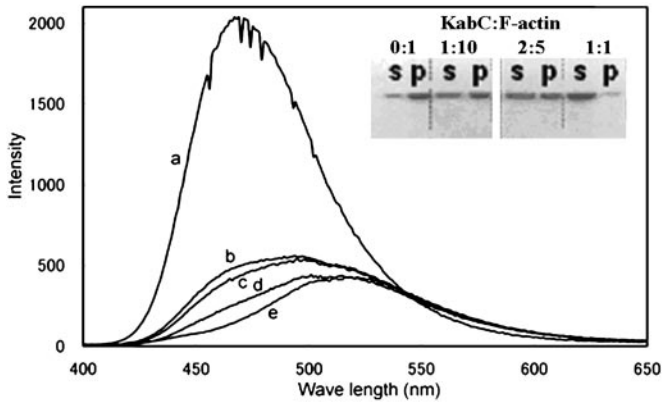


**Fig. 6.** (Trace a) Fluorescence emission spectra of 5 $\mu$M Prodan-F-actin in the absence and after adding KabC to 5 $\mu$M at the following times: 30 sec (trace b), 15 min (trace c), and 39 min (trace d). (Trace e) The spectrum of the same concentration of the labeled G actin–KabC complex. (*Inset*) SDS/PAGE analysis of KabC severing of F-actin. One hundred microliters of F-actin (10 $\mu$M) was treated with KabC (lane 1, 0 $\mu$M; lane 2, 1 $\mu$M; lane 3, 4 $\mu$M; lane 4, 10 $\mu$M) for 30 min and airfuged at 120,000 $\times$ *g* for 30 min. Supernatant (S) and pellet (P) of each sample are shown.

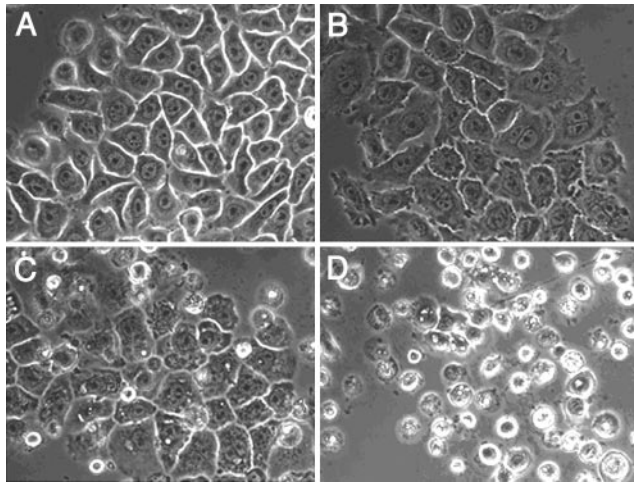


**Fig. 7.** Effect of KabC on NBT-II cells. NBT-II cells imaged after 16 h of drug treatment are shown. KabC concentrations are as follows: control (*A*); 10 nM (*B*); 100 nM (*C*); and 1,000 nM (*D*). Cell death occurs in *D* within ≈8–12 h. At ≈10–100 nM (*B* and *C*), the drug causes an increase in the number of blebs, a breakdown in the Adherens junction, and a cytokinesis defect, as can be seen by the presence of two to four nuclei, whereas control cells harbor a single nucleus. At 100 nM, the cells lose control of contractile functions and have enlarged vesicles.

quantum yield is directly related to filament severing is neither justified nor validated in these studies. As we show below, the decrease in the fluorescence could also be caused by an immediate, macrolide-induced perturbation of the molecular environment around the probe that is unrelated to filament severing.

As expected, the addition of an equimolar amount of KabC to Prodan-F-actin leads to an immediate decrease in the quantum yield. This is followed by a far slower red-shift in the average energy of the emission spectrum over time that after 40 min has still not reached the value seen for free Prodan-G-actin or the Prodan-G-actin–KabC complex (Fig. 2*A*, traces a and n). This result suggests that the immediate quenching of fluorescence by equimolar KabC cannot be used as a measure of F-actin depolymerization and the formation of the G-actin–KabC complex. The emission spectrum of Prodan-F-actin treated with a substoichiometric amount of KabC (one tenth) is very similar to the control Prodan-F-actin and does not shift appreciably in time (data not shown). This result demonstrates that F-actin is not depolymerized by substoichiometric amounts of KabC, as might be expected for a drug that engages in multiple binding and severing events. Further proof that the fluorescence quenching and filament severing events are uncoupled is shown in an SDS/PAGE analysis of the same Prodan-F-actin/KabC mixtures. In this experiment, the monomeric actin (supernatant, S) and F-actin (pellet, P) fractions of KabC treated F-actin are separated by high-speed centrifugation (120,000 $\times$ *g*) and quantified by staining of the gel. In the samples containing F-Actin/KabC in the ratio of 10:1 and 5:2, we find that a significant fraction of the total actin exists as F-actin (Fig. 6 *Inset*). If KabC were to engage in multiple binding and severing events with the filament, then the majority of the actin in these samples would appear in the supernatant fraction as either monomers or short filaments. Furthermore, we deduce from these particular data that KabC-mediated severing is slow, otherwise most of the actin would be present in the supernatant fraction (e.g., in Fig. 6 *Inset*, the average filament length would contain 2.5 actin protomers). Together these studies show that, although KabC binds rapidly to Prodan-F-actin, it triggers a single and slow severing event: the KabC remains strongly bound to this actin protomer, which defines the (+) end and blocks further filament growth.

From our analyses of the interaction of KabC with F- and G-actin using fluorescence assays and kinetic, SDS/PAGE, and structural studies reported by Klenchin *et al*. (17), we propose a two-step reaction mechanism to explain the severing of actin filaments by KabC and related macrolides (summarized in Fig. 8*C*, which is published as supporting information on the PNAS web site). First, the macrolide ring of KabC binds rapidly to the exposed hydrophobic patch on an actin protomer in the filament. Consistent with this hypothesis, structural models show that the macrolide ring-binding site on actin protomers is fully exposed within the actin filament (17). The rapid binding of KabC to Prodan-F-actin immediately decreases the quantum yield of Prodan (presumably the same holds true for pyrene-F-actin); however, this rapid primary binding event does not sever the actin filament. Second, the bound macrolide ring positions the KabC tail so that it can compete for the binding site within the cleft between domains 1 and 3 with the axial actin protomer. This reaction is slow but eventually the KabC tail displaces the hydrophobic plug of the axial actin protomer, which weakens the interaction between adjacent protomers and severs at that site (17). KabC remains strongly bound to the protomer at the (+) end of the severed filament. The macrolide remains strongly bound to the actin protomer at the (+) end of the severed filament. KabC bound to this (+)-end protomer prevents further elongation and functions as an unregulated, (+)-end-capping protein. These severing and capping activities are very similar to Gelsolin, and on this basis we propose that the free form of KabC and related macrolides function as small molecule biomimetics of Gelsolin.

**KabC and Related Macrolides Exhibit Concentration-Dependent Phenotypes.** The cytotoxicity of KabC, UlaA, Hal, MisA, and SwiA is concentration dependent. These results are summarized for KabC treated NBT-II rat bladder carcinoma cells shown in Fig. 7. Cells treated with KabC or related macrolides at a concentration of 1 $\mu$M or higher experience a complete breakdown of their actin cytoskeleton and die within a few hours (Fig. 7*D* and ref. 38). Cells treated with ≈10–100 nM KabC show cytoskeleton-linked phenotypes that include a loss of actin associated with cell–cell contacts, defective cytokinesis as revealed by polyploidy, an increase in the size and number of vacuoles, the loss of cell motility, cell blebbing, and accumulation of F-actin at the cell cortex (Fig. 7 *C* and *D* and data not shown). These phenotypes are not observed in untreated cells.

We interpret these concentration-dependent effects as follows: the free form of the drug enters the cell and, at high concentration, disassembles the actin cytoskeleton through a combination of actin filament severing and G-actin monomer sequestering while the G-actin–KabC complex blocks the (+)-end growth of actin filaments. At a lower concentration, the drug exerts its cytotoxic effects through the stable G-actin monomer complex, which binds to the (+) end of an elongating filament and blocks further growth. This inhibition of actin filament growth has a dramatic effect on cell protrusion (4, 7), cytokinesis (39), and intracellular vesicle transport (40). We propose that the unregulated capping activity of the G-actin–KabC complex prematurely caps elongating filaments during these cellular processes, which leads to shorter dysfunctional actin filaments.

**On the Presence of High Levels of Actin-Directed Macrolides in Nudibranch and Sponge.** Ulapualide A ("red flower" in the Hawaiian language) was discovered in the egg mass of certain species of nudibranch (13). UlaA most likely acts as a chemical defense for the vulnerable eggs against would-be predators. An egg mass weighing 120 g yields up to 30 mg of pure KabC and related trisoxazole macrolides (11). This amount would correspond to an intracellular macrolide concentration of 250 $\mu$M, or $\approx$10,000 times the $IC_{50}$ for mammalian cells. So why doesn't this high level of KabC inhibit the functions of nudibranch actin? We speculate that specific amino acid mutations in nudibranch actin serve to reduce the affinity for KabC by $>10^4$-fold. On the basis of our high-resolution structure for the KabC–actin complex (17) and the thermodynamic and kinetic data presented in this article, we hypothesize that these mutations should exist at sites linked to the binding of the macrolide ring; i.e., Ile-341, Ile-345, Ser-348, and Leu-349, and possibly one or two residues in the cleft between subdomains 1 and 3. Together these mutations would serve to (*i*) significantly decrease the affinity of macrolide ring for the hydrophobic patch on actin, and (*ii*) significantly decrease the probability for the interaction of the KabC tail with the actin cleft.

**Marine Organisms Contain a Large Number of Structurally and Functionally Related Inhibitors of Actin Filament Dynamics.** A review of the literature and a screen of chemical databases shows that, although all of the putative actin-binding drugs contain a macrolide ring, the nature and position of the side groups and the size of the ring varies considerably (Fig. 1). For example, we show in Fig. 1 that the scytophycins (41), typified by tolytoxin (42), have a smaller macrolide ring and lack the trisoxazole moiety. Other classes of macrolide that lack a trisoxazole group, shown in Fig. 1, include aplyronines (43), sphinxolides (44), and reidispongiolides (45). This structural variability suggests that the initial binding reaction is mediated by only a few key contacts between the macrolide ring and the hydrophobic patch on actin that may lead to the discovery of structurally less complicated chemical mimetics from a chemical combinatorial library. All of the macrolide drugs identified from our search of related structures contain a hydrophobic tail of identical length with similarly disposed apolar side groups. Interestingly, our structural studies suggest that this preferred stereochemistry is dictated by the allowable interactions of the apolar groups in the tail within the actin cleft (17). We speculate that the slow binding of the tail within the cleft is associated with conformational transitions in actin that must occur to accommodate these apolar groups. Furthermore, we hypothesize that these slower binding events serve to kinetically trap the macrolide and account for the remarkable stability and lifetime of actin–macrolide complex.

**Summary.** This work has established that members of the trisoxazole macrolide family and related drugs inhibit actin filament dynamics through novel mechanisms summarized in Fig. 8. Knowledge of the structural principles governing the interactions of macrolides with actin together with a understanding of their cytotoxicity will prove useful in designing related classes of natural and synthetic drugs to study the regulation of actin filament dynamics in motile cells and could lead to the development of a new class of biomimetic therapeutics to treat tumor metastasis, cystic fibrosis, organ infarction, glaucoma, and other diseases caused by dysfunctional regulation of the actin cytoskeleton or through complications resulting from the extracellular release of actin.


1. Bamburg, J. R. & Wiggan, O. P. (2002) *Trends Cell Biol.* **12,** 598–605.
2. Asch, H. L., Head, K., Dong, Y., Natoli, F., Winston, J. S., Connolly, J. L. & Asch, B. B. (1996) *Cancer Res.* **56,** 4841–4845.
3. Barkalow, K., Witke, W., Kwiatkowski, D. J. & Hartwig, J. H. (1996) *J. Cell Biol.* **134,** 389–399.
4. Theriot, J. A. & Mitchison, T. J. (1991) *Nature* **352,** 126–131.
5. Cooper, J. A. & Schafer, D. A. (2000) *Curr. Opin. Cell Biol.* **12,** 97–103.
6. Pollard, T. D. (2003) *Nature* **422,** 741–745.
7. Witke, W., Sutherland, J. D., Sharpe, A., Arai, M. & Kwiatkowski, D. J. (2001) *Proc. Natl. Acad. Sci. USA* **98,** 3832–3836.
8. Forscher, P. & Smith, S. J. (1988) *J. Cell Biol.* **107,** 1505–1516.
9. Roy, P., Rajfur, Z., Jones, D., Marriott, G., Loew, L. & Jacobson, K. (2001) *J. Cell Biol.* **153,** 1035–1048.
10. Marriott, G., Miyata, H. & Kinosita, K. (1992) *Biochem. Int.* **26,** 943–951.
11. Matsunaga, S., Fusetani, N., Hashimoto, K., Koseki, K. & Noma, M. (1986) *J. Am. Chem. Soc.* **108,** 847–849.
12. Wada, S., Matsunaga, S., Saito, S., Fusetani, N. & Watabe, S. (1998) *J. Biochem.* **123,** 946–952.
13. Roesener, J. A. & Scheuer, P. J. (1986) *J. Am. Chem. Soc.* **108,** 846–847.
14. Bubb, M. R., Spector, I., Bershadsky, A. D. & Korn, E. D. (1995) *J. Biol. Chem.* **270,** 3463–3466.
15. Saito, S. & Karaki, H. (1996) *Clin. Exp. Pharm. Physiol.* **23,** 743–746.
16. Terry, D. R., Spector, I., Higa, T. & Bubb, M. R. (1997) *J. Biol. Chem.* **272,** 7841–7845.
17. Klenchin, V. A., Allingham, J. S., King, R., Tanaka, J., Marriott, G. & Rayment, I. (2003) *Nat. Struct. Biol.* **10,** in press.
18. Choidas, A., Jungbluth, A., Sechi, A., Murphy, J., Ullrich, A. & Marriott, G. (1998) *Eur. J. Cell Biol.* **77,** 81–90.
19. Marriott, G., Zechel, K. & Jovin, T. M. (1988) *Biochemistry* **27,** 6214–6220.
20. Jefford, C. W., Bernardinelli, G., Tanaka, J. & Higa, T. (1996) *Tetrahedron Lett.* **37,** 159–162.
21. Kobayashi, M., Tanaka, J., Katori, T., Miki, M., Yamashita, M. & Kitagawa, I. (1990) *Chem. Pharm. Bull.* **38,** 2409–2418.
22. Tanaka, J., Higa, T., Kobayashi, M. & Kitagawa, I. (1990) *Chem. Pharm. Bull.* **38,** 2967–2970.
23. Heidecker, M., Yan-Marriott, Y. & Marriott, G. (1995) *Biochemistry* **34,** 11017–11025.
24. Zechel, K. (1993) *Biochem. J.* **290,** 411–417.
25. Johnson, N., Marriott, G. & Weber, K. (1988) *EMBO. J.* **7,** 2435–2442.
26. McLaughlin, P. J., Gooch, J. T., Mannherz, H. G. & Weeds, A. G. (1993) *Nature* **364,** 685–692.
27. Doi, Y., Banba, M. & Vertut-Doi, A. (1991) *Biochemistry* **30,** 5769–5777.
28. Kouyama, T. & Mihashi, K. (1981) *Eur. J. Biochem.* **114,** 33–38.
29. Cooper, J. A., Walker, S. B. & Pollard, T. D. (1983) *J. Muscle Res. Cell Motil.* **4,** 253–262.
30. Macgregor, R. B. & Weber, G. (1986) *Nature* **319,** 70–73.
31. Weber, G. & Farris, F. J. (1979) *Biochemistry* **18,** 3075–3078.
32. Janmey, P. A., Chaponnier, C., Lind, S. E., Zaner, K. S., Stossel, T. P. & Yin, H. L. (1985) *Biochemstry* **24,** 3714–3723.
33. Janmey, P. A., Iida, K., Yin, H. L. & Stossel, T. P. (1987) *J. Biol. Chem.* **262,** 12228–12236.
34. Chen, P., Murphy-Ullrich, J. E. & Wells, A. (1996) *J. Cell Biol.* **134,** 689–698.
35. Botelho, R. J., Teruel, M., Dierckman, R., Anderson, R., Wells, A., York, J. D., Meyer, T. & Grinstein, S. (2000) *J. Cell Biol.* **151,** 1353–1368.
36. Kabsch, W., Mannherz, H. G., Suck, D., Pai, E. F. & Holmes, K. C. (1990) *Nature* **347,** 37–44.
37. Morton, W. M., Ayscough, K. R. & McLaughlin, P. J. (2000) *Nat. Cell Biol.* **2,** 376–378.
38. Spector, I., Braet, F., Shochet, N. R. & Bubb, M. R. (1999) *Microsc. Res. Tech.* **47,** 18–37.
39. Guertin, D. A., Trautmann, S. & McCollum, D. (2002) *Microbiol. Mol. Biol. Rev.* **66,** 155–178.
40. Rozelle, A. L., Machesky, L. M., Yamamoto, M., Driessens, M. H. E., Insall, R. H., Roth, M. G., Luby-Phelps, K., Marriott, G., Hall, A. & Yin, H. L. (2000) *Curr. Biol.* **10,** 311–320.
41. Ishibashi, M., Moore, R. E., Patterson, G. M. L., Xu, C. & Clardy, J. (1986) *J. Org. Chem.* **51,** 5300–5306.
42. Carmeli, S., Moore, R. E. & Patterson, G. M. L. (1990) *J. Nat. Products* **53,** 1533–1542.
43. Yamada, K., Ojika, M., Ishigaki, T., Yoshida, Y., Ekimoto, H. & Arakawa, M. (1993) *J. Am. Chem. Soc.* **115,** 11020–11021.
44. Guella, G., Mancini, I., Chiasera, G. & Pietra, F. (1989) *Helv. Chim. Acta* **72,** 237–246.
45. D'Auria, M. V., Paloma, L. G., Minale, L., Zampella, A., Verbist, J.-F., Roussakis, C., Debitus, C. & Patissou, J. (1994) *Tetrahedron* **50,** 4829–4834.